JOURNAL OF APPLIED ELECTROCHEMISTRY **27** (1997) 1349–1354

# Production and properties of electrolytic Ni–P–TiO$_2$ composite layers

D. GIERLOTKA, E. RÓWIŃSKI, A. BUDNIOK, E. ŁAGIEWKA

*Institute of Physics and Chemistry of Metals, University of Silesia, Pl-40-007 Katowice, Bankowa 12 Poland*

Received 5 March 1996; revised 7 May 1997

Ni–P–TiO$_2$ active cathodes were prepared by simultaneous electrodeposition of Ni and TiO$_2$ on a Cu substrate from a solution in which TiO$_2$ particles were suspended by stirring. Electrodeposition was carried out under galvanostatic conditions at a current density of 240 mA cm$^{-2}$ for 0.5 h. For comparison, Ni–P layers were also obtained under the same conditions. Following heat treatment in air two further types of electrode material were obtained. X-ray diffractometer, scanning electron microscope, X-ray probe microanalyser, Auger spectroscope and atomic absorption spectroscope were used for physical and chemical characterization of the layers. It was ascertained that the introduction of TiO$_2$ to the amorphous Ni–P layers leads to an increase in the rate of hydrogen evolution in comparison with conventional Ni–P layers irrespective of environment. Heat treatment does not exert an appreciable influence on the rate of hydrogen evolution on a Ni–P electrode and induces a slight inhibition of hydrogen evolution on a Ni–P–TiO$_2$ electrode in acid environment.

Keywords: *composite layers*, *electrode materials*

## 1. Introduction

Recently, electroactive Ni–RuO$_2$ materials were obtained by codeposition of nickel in a Watts bath in which RuO$_2$ particles were dispersed and suspended by intensive mixing [1, 2]. The catalytic activity of these materials appeared to depend on the RuO$_2$ content in the layer and the overpotential of hydrogen evolution on such electrode materials was not large. The feasibility of utilizing such electrodes for chlor-alkali electrolysis was indicated on a laboratory scale.

Electrodes containing titanium and its oxides are already widely applied (e.g. ruthenium–titanium oxide anodes [3]), iridium–titanium oxide anodes [4], iridium–ruthenium–titanium oxide anodes [5, 6]. Ceramic oxide electrodes based on a Ti/TiO$_2$ system also find application in electrochemical synthesis [7–15].

The objective of the present work was to obtain amorphous Ni–P layers containing crystalline TiO$_2$, to investigate their properties and the influence of heat treatment on the layer structure, and finally to evaluate their potential as electrode materials for electrolytic hydrogen evolution in acid and alkaline environments. The choice of the type of matrix and the component was based on earlier positive tests of their individual electrocatalytic behaviour in certain electrochemical processes [16].

## 2. Experimental details

To obtain composite Ni–P–TiO$_2$ layers on a copper substrate, the following electrolyte was prepared (g dm$^{-3}$): 51 – NiSO$_4$.7H$_2$O, 107 – NH$_4$Cl, 29 – NaH$_2$PO$_2$.H$_2$O, 8 – H$_3$BO$_3$ and 10 – CH$_3$COONa to which 200 g dm$^{-3}$ TiO$_2$ (anatase) was added. The granulometry of TiO$_2$ particles estimated by the optical method (magnification 500×) was 5–15 × 10$^{-6}$ m. Reagents from POCh Gliwice (Poland) of analytical purity and deionized water were used for the solution, pH of the suspension was 4.8–5.1.

A copper substrate was polished mechanically on abrasive paper and using diamond pastes, and then electrolytically, in order to remove the layer deformed by mechanical treatment. Electrolytic polishing was carried out as described in [17]. The copper plates of one-sided area 1 cm$^2$ were placed parallel to the bottom of the vessel ($V$ = 400 cm$^3$). The other side of the plates was covered with nonconducting resin. The distance between the plates and the surface of the solution was 5 cm. A platinum mesh was used as counter electrode (1 dm$^2$). The process was carried out at 298 K and current density 240 mA cm$^{-2}$ for 0.5 h, with intensive mechanical mixing of the bath (300 rpm). The Ni–P alloy was obtained under the same conditions from a nickel-plating bath yet devoid of TiO$_2$. The thickness of the deposited layers, estimated by weighing, was found to be about 25 $\mu$m.

Following heat treatment in air at 673 K for 0.5 h two further electrode materials exhibiting crystalline structure were obtained.

Quantitative chemical analysis of the layers was carried out by atomic absorption spectroscopy (AAS) using a Perkin–Elmer spectrometer. For this purpose the layers were solubilized in a hydrochloric acid solution (1:1 v/v) with the addition of few drops of nitric acid, and then, after suitable dilution, the nickel and titanium were determined. Error in determination was estimated at about 3% for both Ni and Ti. The phosphorus content was estimated indirectly by determining the molybdenum content in the previously formed phosphoromolybdenic acid. The determination error was estimated at about 3%. From results obtained, and making use of the stoichiometric relations and the gain in weight of the layers together with phase analysis results, the $TiO_2$ content of the layers was calculated.

The surface morphology of both Ni–P–$TiO_2$ and Ni–P layers was examined by means of a scanning electron microscope (SEM, JXA-50A). The surface distributions of Ni and Ti were investigated by means of an X-ray microanalyser JXA-50A. The Auger electron spectroscope SEA02 was used to determine the depth profile of chemical composition of the layers. Structural compositions of the layers were determined by X-ray diffraction using a Philips diffractometer and Cu$K_\alpha$ radiation.

Electrochemical investigations were carried out in a three-electrode vessel using an EP-20 potentiostat and a GSTP-3 generator. The reference electrode was a saturated calomel electrode (SCE), and the auxiliary electrode was a platinum mesh of total area 1 $dm^2$. Tests were conducted in both a 2.5 M $H_2SO_4$ solution and a 2.5 M NaOH solution at 298 K. Electrochemical characteristics of the layers were determined after prior cyclic activation by a saw-shaped polarization impulse in the direction of hydrogen evolution. The scan rate was 20 mV $s^{-1}$. Cycling was continued for 3 h and an increase in electrode activity was found, as indicated by the rising values of current after each cycle at comparable potentials. Then the final *j–E* relation was recorded for each sample at a scan rate of 20 mV $s^{-1}$. From the curves obtained, and after converting the potential to the hydrogen electrode scale, the rates of hydrogen evolution on various materials were compared.

## 3. Results and discussion

The electrolytic composite Ni–P–$TiO_2$ layers and the Ni–P layers exhibit good adherence to the copper substrate and can be deposited up to a thickness of 25 $\mu$m. The layers of Ni–P–$TiO_2$ contain 52.6% Ni, 23.2% P and 24.2% $TiO_2$ and the Ni–P layers obtained in the same conditions contain 71.2% Ni and 28.8% P.

The diffractograms of these layers show that Ni–P–$TiO_2$ layer exhibits a matrix corresponding to the amorphous Ni–P layer and an additional crystalline $TiO_2$ phase (Fig. 1(a) and (b)). This means that during the electrodeposition process a spherical crystalline particle is incorporated into the Ni–P phase matrix. Thermal treatment of both the Ni–P–$TiO_2$ and Ni–P layers leads to crystallization of the amorphous matrix so that, in effect, apart from the nickel crystallites, nickel phosphide $Ni_5P_2$ is also present (Fig. 1(c) and (d)).

The surface layer of Ni–P differs from that of Ni–P–$TiO_2$ by the presence of microcracks, which probably increase the roughness factor (Fig. 2(a) and (b)). The presence of $TiO_2$ in the Ni–P layer affects heterogeneity of the surface and increases the number of boundaries between Ni and other particles in the matrix.

The surface distribution of nickel and titanium in the Ni–P–$TiO_2$ layers is virtually homogeneous which is due to a molecular mixing of the amorphous nickel matrix with the particles of titanium oxide (Fig. 3(a) and (b)).

Using the Auger spectroscopy it was found that after etching for about 40 min with argon atoms the surface layer exhibits stability of the chemical composition, with phosphorus, titanium, nickel, carbon and oxygen present in the layers (Fig. 4). Assuming that oxygen coexists only with titanium the stoichiometric formula of titanium oxide as $Ti_2O_3$ was ascertained. Both the process of codeposition of nickel with $TiO_2$ and the reaction of $NaH_2PO_2$ and $Ni^{2+}$ ions to form $Ni_5P_2$ may also favour the surface reduction of $TiO_2$ to afford nonstoichiometric titanium oxides like $Ti_2O_3$. However, in the X-ray phase analysis this phase was not found which could mean that this phase is either amorphous or its amount is too small to be detectable by the X-ray phase analysis. Nevertheless, a system of nonstoichiometric titanium oxides coexists in the surface layer, a fact which may be of considerable significance when it is used as an electrode material.

The *j–E* relations characterizing the behaviour of the Ni–P–$TiO_2$ and Ni–P layers in an acid environment exhibit a very similar form irrespective of heat treatment (Fig. 5). In each case the electrode process is associated with the evolution of hydrogen. The layers containing $TiO_2$ at comparable potentials exhibit a higher rate of the hydrogen evolution than the layers without $TiO_2$ (Fig. 5 curves 1 and 3). At a potential $E = -0.300$ V the rate of hydrogen evolution is in this case about five times greater than on the electrode without $TiO_2$ and equals $j_1 = 230$ mA $cm^{-2}$. This value of current density occurs on the Ni–P electrode after increase in its polarization to $E = -0.560$ V. It means that the introduction of $TiO_2$ into the amorphous Ni–P matrix induces easier depolarization of the hydrogen ions on the electrode which has the value of about 0.260 V less than for the Ni–P one. This implies that the rate of hydrogen evolution on the Ni–P–$TiO_2$ electrode in acid environment is greater than on the Ni–P electrode. In the aggregate this may suggest the participation of titanium oxides in the electrochemical surface reactions taking place during hydrogen evolution. In acid media the $TiO_2$ particles on the surface of the electrode exist in the protonated state or in a redox form [15]:

$$TiO_2 + H^+ \Leftrightarrow TiOOH^+ \tag{1}$$

$$2\ TiO_2 + 2H^+ + 2e^- \Leftrightarrow 2\ TiOOH \Leftrightarrow Ti_2O_3 + H_2O \tag{2}$$

The hydrogen ions can easily interact:

$$TiOOH^+ + H^+ + 2e^- \Longrightarrow TiO_2 + H_2 \tag{3}$$

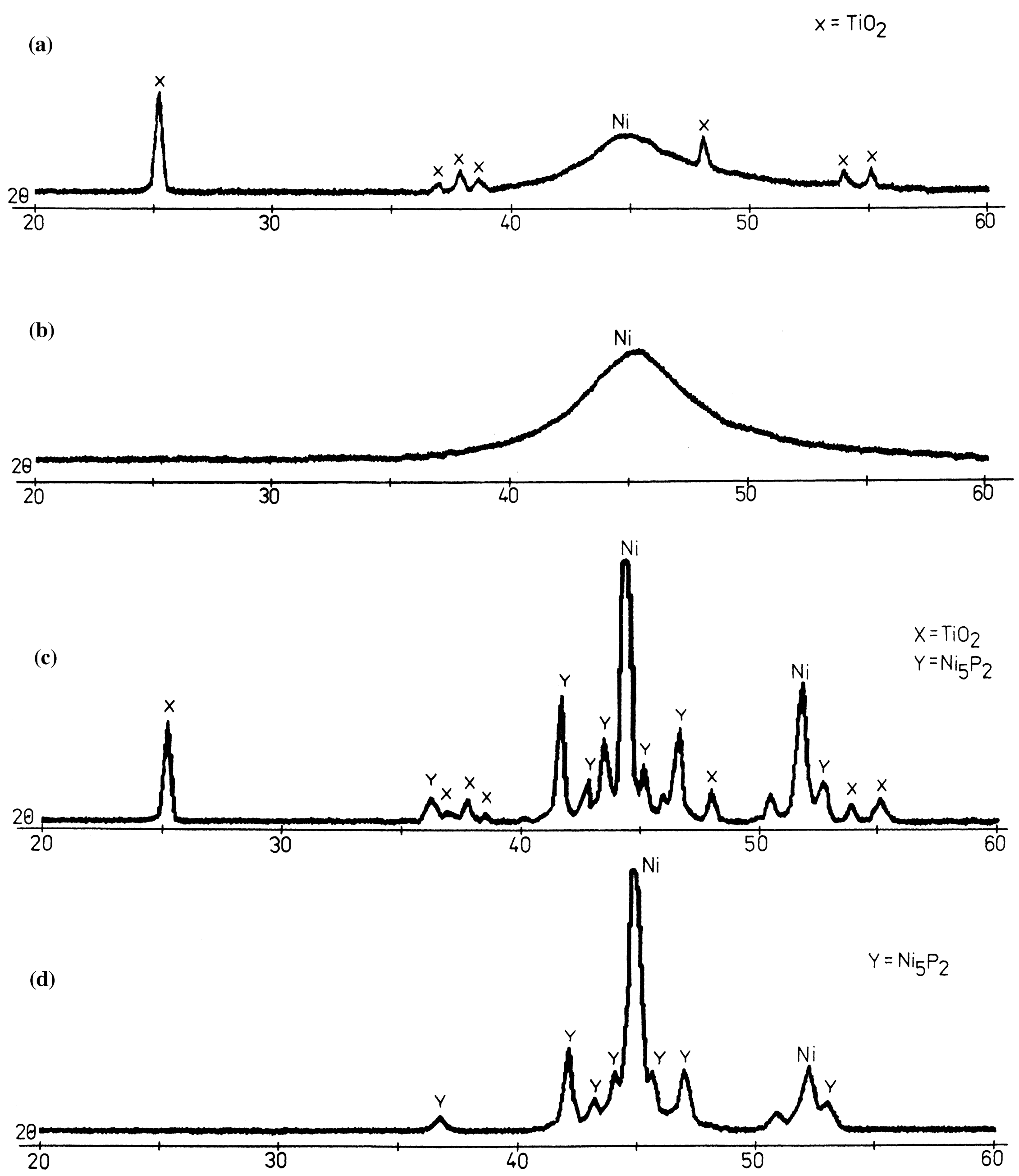

Fig. 1. X-ray diffraction pattern: (a) Ni–P–TiO$_2$, (b) Ni–P, (c) Ni–P–TiO$_2$ after heat treatment, (d) Ni–P layer after heat treatment.

or

$$2\ \mathrm{TiOOH}\ + 2\mathrm{H}^+ + 2\mathrm{e}^- \Longrightarrow 2\ \mathrm{TiO}_2 + 2\mathrm{H}_2 \qquad (4)$$

Summing Equations 1 and 3 or 2 and 4 the following relation is obtained:

$$2\mathrm{H}^+ + 2\mathrm{e}^- \Longrightarrow \mathrm{H}_2 \qquad (5)$$

Similar catalytic hydrogen evolution was observed by the reduction of aromatic nitro compounds in $H_2SO_4$ [15].

Heat treatment influences the course of the hydrogen evolution process in the Ni–P–TiO$_2$ layers and also causes no apparent change in the *j–E* relations (Fig. 5 curves 3, 4). At the potential $E = -0.300$ V the rate of hydrogen evolution is equal to about 90% of the $j_1$. This indicates that in this case heat treatment of the material induces a slight inhibition of the hydrogen evolution from an acid environment. Subjecting the Ni–P layers to heat treatment intensifies the hydrogen evolution (Fig. 5 curves 1, 2). At the potential $E = -0.300$ V the rate of hydrogen evolution is about two times greater in comparison to the electrode with the same potential but not subjected to thermal treatment and is equal to $j_2 = 100\ \mathrm{mA\,cm^{-2}}$. This value of current density occurs on the Ni–P electrode without thermal treatment after increasing the polarization of the electrode to $E = -0.400$ V. Hence in this case heat treatment has an advantageous effect on the course of the electrolytic evolution of hydrogen in the Ni–P layer from an acid environment.

The *j–E* curves characterizing the behaviour of the Ni–P–TiO$_2$ and Ni–P layers in an alkaline environment have a very similar form, irrespective of heat

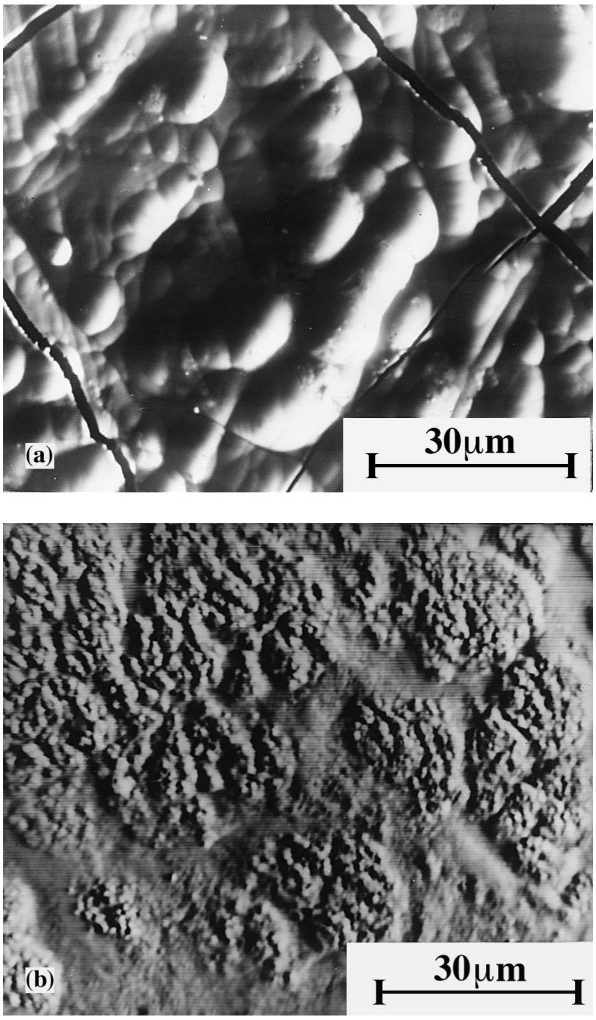

Fig. 2. Scanning electron micrographs of Ni–P (a) and Ni–P–$TiO_2$ (b) layers.

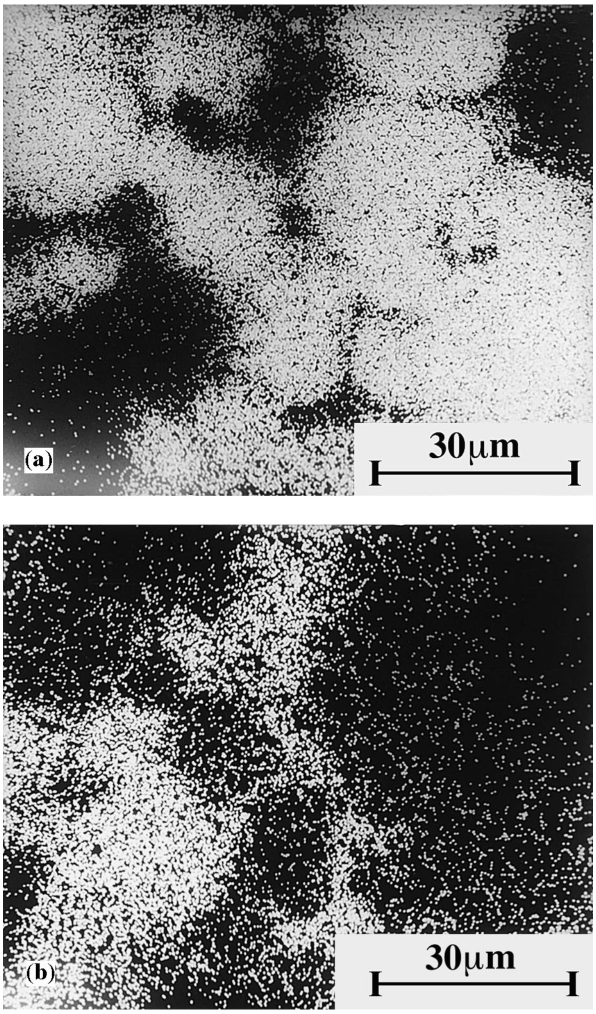

Fig. 3. Surface distribution of nickel (a) and titanium (b) in the Ni–P–$TiO_2$ layer after deposition. (The SEM picture (Fig. 2) and the surface distributions of Ni and Ti cover the same position on the specimen surface.)

treatment (Fig. 6). In each case the process taking place is associated with the reduction of water molecules and evolution of hydrogen. Comparison of the curves obtained for both the Ni–P and Ni–P–$TiO_2$ layers shows that at comparable potentials the layers containing $TiO_2$ exhibit a more rapid electrode process than those not containing $TiO_2$ (Fig. 6 curves 1, 3). Thus the presence of $TiO_2$ in the amorphous Ni–P matrix promotes hydrogen evolution. Taking into consideration the equilibrium potential of the hydrogen electrode in alkaline environment ($E = -0.828\,\mathrm{V}$) [18] and the value of the SCE potential (0.244 V) [18], the rates of hydrogen evolution at the overpotential $\Delta E_1 = -0.300\,\mathrm{V}$ and at $\Delta E_2 = -0.500\,\mathrm{V}$ were determined. At the overpotential $\Delta E_1$ the rate of hydrogen evolution is greater on the Ni–P–$TiO_2$ layer than on the electrode without $TiO_2$ and is equal to $j_3 = 70\ \mathrm{mA\,cm^{-2}}$. This value of current density occurs on the Ni–P electrode after increasing the polarization of the electrode to $\Delta E = -0.500$ V. At the overpotential $\Delta E_2$ the rate of hydrogen evolution is greater on the Ni–P–$TiO_2$ layer than on the electrode without $TiO_2$ and is equal to $j_4 = 175\,\mathrm{mA\,cm^{-2}}$. This value of current density occurs on the Ni–P electrode after increasing polarization of the electrode to $\Delta E = -0.750$ V which implies that the introduction of $TiO_2$ into the amorphous Ni–P matrix induces easier depolarization of the water molecules. This may suggest the participation of titanium oxides in the electrochemical surface reactions taking place during the hydrogen evolution from an alkaline environment. The $TiO_2$ particles on the surface of the electrode exist in redox system $TiO_2 \Leftrightarrow Ti_2O_3 \Leftrightarrow 2\,TiOOH$. The presence of such phases evokes the electrocatalytic effect during hydrogen evolution.

$$TiO_2 + H_2O + e^- \Longrightarrow TiOOH + OH^- \qquad (6)$$

$$TiOOH + H_2O + e^- \Longrightarrow TiO_2 + H_2 + OH^- \qquad (7)$$

Summing up, the following relation is obtained:

$$2\,H_2O + 2e^- \Longrightarrow H_2 + 2\,OH^- \qquad (8)$$

The rate of hydrogen evolution determined in the overpotential interval of 0.410–0.620 V in 6 M KOH for steel and Ni–Cr, Ni–Fe, Ni–W layers in an alkaline environment is equal to about $j = 250$–300 $\mathrm{mA\,cm^{-2}}$ and for a nickel electrode in 30% KOH at

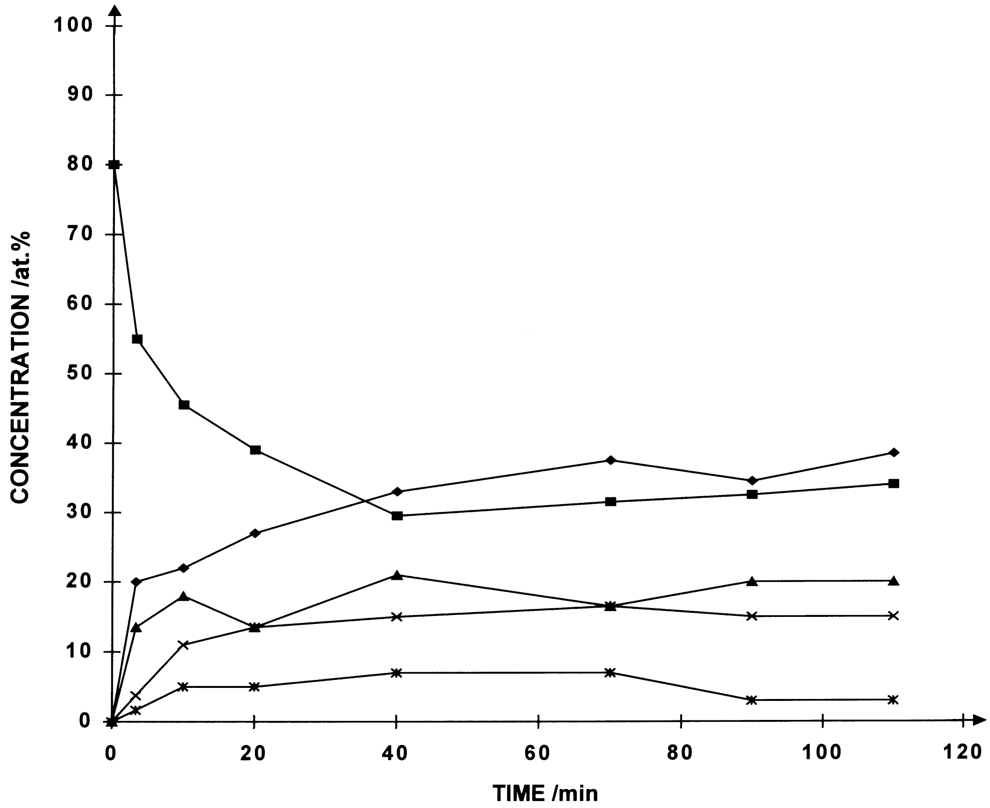

Fig. 4. Depth profile of the Ni–P–TiO$_2$ layer depending on sputtering time by means of argon ions (4 kV, 0.76 $\mu$A mm$^{-2}$). Key: (◆) O, (■) C, (▲) Ni, (×) Ti and (*) P.

$\Delta E = -0.510$ V is equal to about $j = 250$ mA cm$^{-2}$ [19]. Thus it is clear that the rate of hydrogen evolution in these investigations is smaller than for a nickel electrode and is comparable with the values obtained for other materials envisaged for electrolytic hydrogen evolution [19, 20].

After heat treatment of the Ni–P–TiO$_2$ layers a decrease of the hydrogen evolution was observed (Fig. 6 curves 3, 4). The influence of heat treatment on the hydrogen evolution process on the Ni–P layers is virtually negligible and exerts no significant effect on the *j–E* relations (Fig. 6 curves 1, 2).

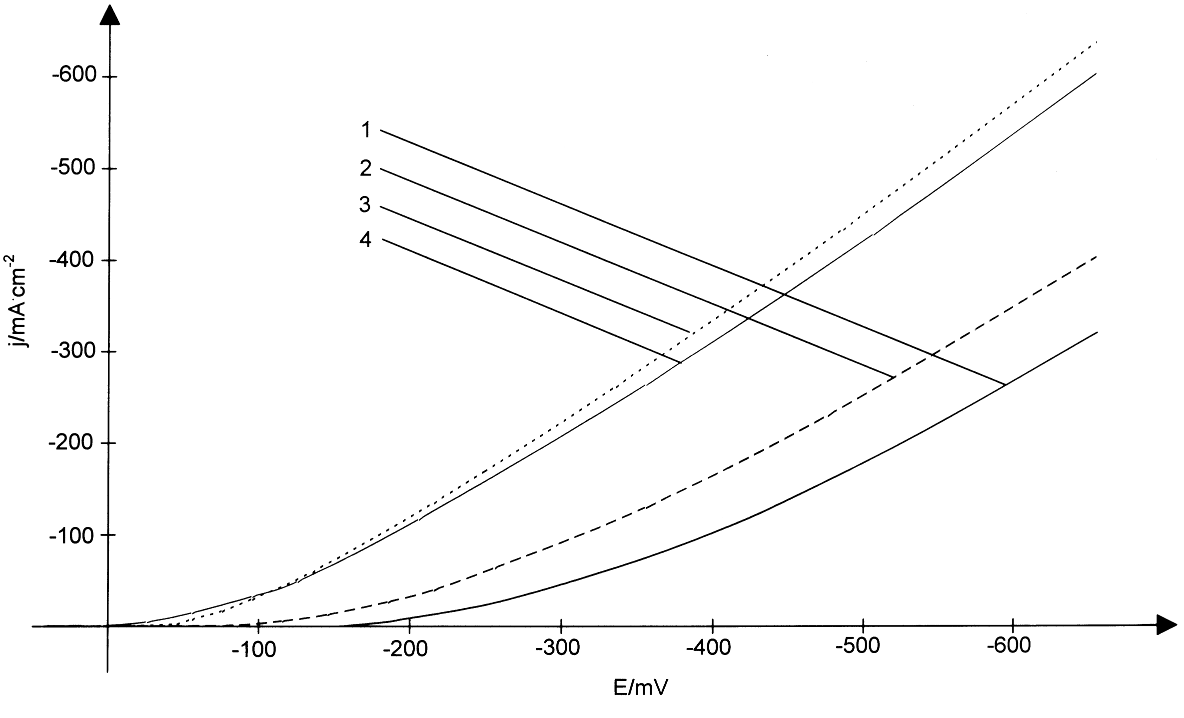

Fig. 5. *j–E* relations obtained in 2.5 M H$_2$SO$_4$ solution: (1) Ni–P, (2) Ni–P after heat treatment, (3) Ni–P–TiO$_2$, (4) Ni–P–TiO$_2$ after heat treatment (Scan rate 20 mV s$^{-1}$).

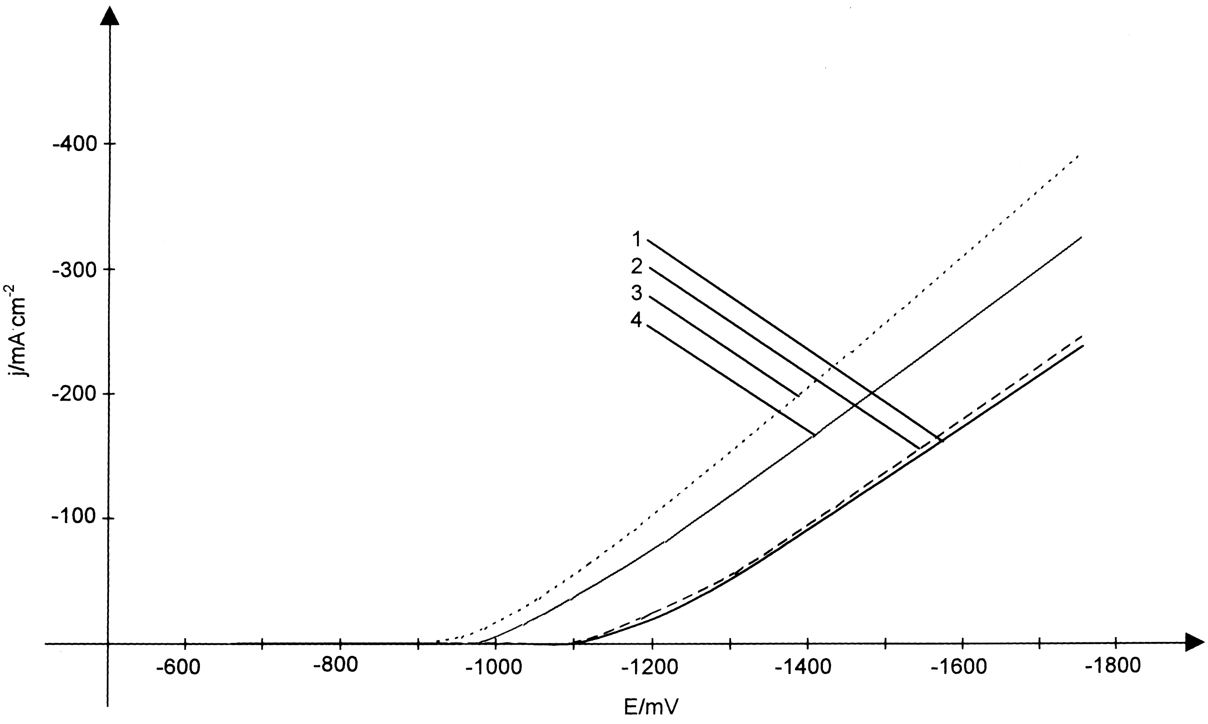

Fig. 6. *j–E* relations obtained in 2.5 M NaOH solution: (1) Ni–P, (2) Ni–P after heat treatment, (3) Ni–P–$TiO_2$, (4) Ni–P–$TiO_2$ after heat treatment (Scan rate 20 mV s$^{-1}$).

## 4. Conclusions

Chemical and phase analysis of the Ni–P–$TiO_2$ layer confirms the codeposition of nickel and $TiO_2$ and the formation of a homogeneous electrode material. Electrolytically deposited composite layers exhibit an amorphous structure of the nickel matrix in which the crystalline titanium oxide $TiO_2$ is incorporated. Heat treatment of these layers leads to the formation of a crystalline layer in which the Ni and $Ni_5P_2$ crystallites appear apart from those of $TiO_2$ (anatase).

The introduction of $TiO_2$ to the amorphous Ni–P layers results in the increase in the rate of hydrogen evolution in comparison with the Ni–P layers and this is observed both in acid and alkaline environment. Hence the evolution of hydrogen on the composite Ni–P–$TiO_2$ layer may be directly associated with the presence of $TiO_2$ and its protonated state or/and redox forms of $Ti_2O_3 \Leftrightarrow$ TiOOH which exert an electrocatalytic effect on the hydrogen evolution process. This agrees with the results obtained by Noel [15]. Heat treatment does not affect appreciably the rate of hydrogen evolution.

## Acknowledgement

This research was partially financed by the Polish Committee for Scientific Research (Project 7 T08B 027 10).

## References

[1] N. Spataru and J.-G. Le Helloco, *Rev. Roum. de Chimie* **40** (1995) 505.

[2] C. Iwakura, M. Tanaka, S. Nakamatsu, H. Inoue, M. Matsuoka and N. Furukawa, *Electrochim. Acta* **40** (1995) 977.

[3] Ya. M. Kolotyrkin, V. V. Losev, D. M. Shub, *Elektrokhimiya* **15** (1979) 291.

[4] Abstracts of Papers 5th All-Union Conference, 'Dimensionally Stable Anodes and their Application in Electrochemical Processes', VINITI, Moscow (1987).

[5] Abstracts of Papers 3rd All-Union Conference on Electrocatalysis, Moscow (1991).

[6] Abstracts of Papers 3rd All-Union Conference on Electrochemisty, VINITI, Moscow (1988) vol. 3.

[7] F. Beck and W. Gabriel, *Angew. Chem.* **24** (1985) 771.

[8] S. E. Lindquist, A. Lindgren and Z. Y. Ning, *J. Electrochem. Soc.* **132** (1985) 623.

[9] R. Piontelli and P. Pedeferri, *Electrochim. Metall.* **3** (1967) 346.

[10] C. Ravichandran, M. Noel, S. Thangavelu and P. N. Anantharaman *J. Electroanal. Chem.* **369** (1994) 217.

[11] C. Ravichandran, D. Vasudevan and P. N. Anantharaman, *J. Appl. Electrochem.* **22** (1992) 179.

[12] D. Vasudevan and P. N. Anantharaman, *ibid.* **24** (1994) 559.

[13] C. Ravichandran, D. Vasudevan, S. Thangavelu and P. N. Anantharaman, *ibid.* **22** (1992) 1087.

[14] D. Vasudevan, S. Chellammal and P. N. Anantharaman, *ibid.* **21** (1991) 839.

[15] M. Noel, C. Ravichandran and P. N. Anantharaman, *ibid.* **25** (1995) 690.

[16] J. ÓM. Bockris and S. U. M. Khan, 'Surface Electrochemistry', Plenum Press, New York (1993).

[17] M. Oleksy, A. Budniok, J. Niedbala and P. Matyja, *Electrochim. Acta* **16** (1994) 2439.

[18] R. Parsons (ed). 'Handbook of Electrochemical Constants', Butterworths Scientific, London (1959).

[19] J. A. Raj and K. I. Vasu, *J. Appl. Electrochem.* **20** (1990) 32.

[20] B. Więcek, *Polish J. Chem.* **69** (1995) 612.